A multichannel shot noise approach to describe synaptic background activity in neurons

M. Rudolph[a] and A. Destexhe

Integrative and Computational Neuroscience Unit, CNRS, Bat. 33, 1 Avenue de la Terrasse,
91198 Gif-sur-Yvette Cedex, France

Abstract. Systems driven by Poisson-distributed quantal inputs can be described as "shot noise" stochastic processes. This formalism can apply to neurons which receive a large number of Poisson-distributed synaptic inputs of similar quantal size. However, the presence of temporal correlations between these inputs destroys their quantal nature, and such systems can no longer be described by classical shot noise processes. Here, we show that explicit expressions for various statistical properties, such as the amplitude distribution and the power spectral density, can be deduced and investigated as functions of the correlation between input channels. The monotonic behavior of these expressions allows an one-to-one relation between temporal correlations and the statistics of fluctuations. Multi-channel shot noise processes, therefore, open a way to deduce correlations in input patterns by analyzing fluctuations in experimental systems. We discuss applications such as detecting correlations in networks of neurons from intracellular recordings of single neurons.

1 Introduction

With first reports dating back to the beginning of the last century [1], the effect originally termed "Schroteffekt" [2] describes spontaneous time-dependent current fluctuations in electric conductors. Such fluctuations, now well-known under the term *shot noise* [3], do have their origin in the quantum mechanical properties of electrons, specifically the discreteness of the electric charge. In contrast to thermal (Johnson-Nyquist) noise [4], the appearance of shot noise is inevitably linked to non-equilibrium states of the system in question.

The inherent quantum nature of shot noise processes led to a generalization of its definition, which describes shot noise as the output $s(t)$ of a dynamical system activated by a sequence $z(t)$ of singular impulses occurring at random times t_i, $s(t) = \sum_i h(t - t_i)$ [5] (Fig. 1A). Here, $h(t)$ denotes the quantal impulse response elicited for each event t_i. In mathematical terms, shot noise processes are strict-sense stationary stochastic processes, i.e. their statistical properties are invariant to shifts in time, for which $s(t)$ can be represented as the output of a linear system with quantal impulse response $h(t)$ and random impulse input $z(t) = \sum_i \delta(t - t_i)$. In general, $z(t)$ is assumed to be a
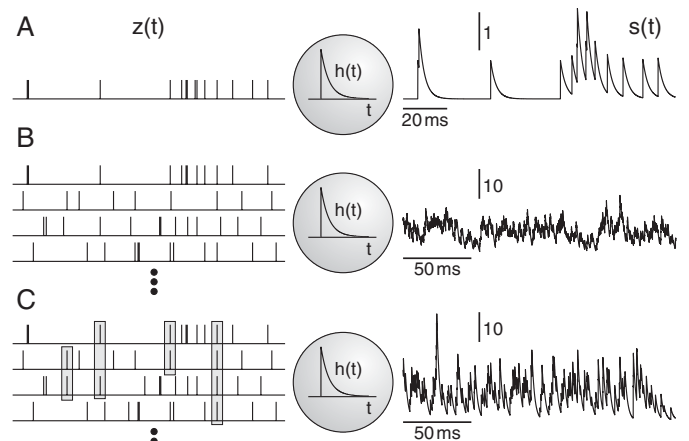
Fig. 1. Shot noise process for single (A), multiple uncorrelated (B) and multiple correlated (C) input channels. The output $s(t)$ of the dynamical system equals the sum of the quantal responses $h(t)$ triggered by the arrival of a sequence of impulses $z(t)$ occurring at random times according to a Poisson distribution. Whereas $s(t)$ triggered by multiple but uncorrelated channels (B) can be described by a single channel with high rate, the output differs when temporal correlations (C, left, grey bars) are introduced. Parameters: $N = 1$, $\lambda = 100$ Hz (A); $N = 100$, $\lambda = 50$ Hz, $c = 0$ (B); $c = 0.7$ (C); $h_0 = 1$, $\tau = 2$ ms in all cases.

[a] e-mail: Michelle.Rudolph@iaf.cnrs-gif.fr

Poisson process of constant rate [3,6], but also cases considering underlying Poisson processes with time-varying rate [7], filtered Poisson processes [8] or Gaussian noise [9] were investigated.

With this generalization, (quantum) shot noise processes have emerged as a theoretical basis for the explanation of a variety of phenomena. These include, most notably, electronic transport phenomena in mesoscopic systems [11], such as the Aharonov-Bohm effect, the quantum Hall effect [10], superconductivity [12], or the kinetics of entangled and spin-polarized electrons [13]. Effects like the diffusion of concentration packets, a specific example of which is synaptic transmission between neurons, are accessible in the framework of power-law or fractal shot noise processes [14,18]. The theory of shot noise processes even found extensions to (quantum) optics [15], risk [16], telecommunication and traffic theory [17].

Campbell's theorem [1,3] provides explicit expressions for the first and second cumulants (mean and variance, respectively) of single-channel Poisson-driven shot noise processes with integrable response functions $h(t)$. However, in many situations, e.g. synaptic transmission in neural systems, the response is triggered by multiple input channels $z_i(t)$. Whereas for N independent input channels with rate λ (Fig. 1B) the resulting output $s(t)$ is equivalent to a single channel driven by a Poisson process of higher rate λN, this generalization is no longer valid in the presence of temporal correlations between the multiple input channels (Fig. 1C). In this paper, we apply Campbell's theorem to situations of multiple and temporally correlated input channels, and provide explicit expressions for various statistical measures, which will allow to characterize the quantal impulse response and input statistics from the sole knowledge of the system's output. We discuss applications of this formalism to model synaptic activity in neurons.

2 Correlated input channels and generalization of Campbell's theorem

Temporal correlation among the multiple input channels was introduced using a *distributed generator algorithm* (Fig. 2A), which was originally proposed to model correlations among multiple synapses in neurons [19]. At each time step t_0, the activity in channel $i = 1, \ldots, N$ (set $\{B\}$) is selected independently and uniformly from one of N_0 independent Poisson trains (set $\{A\}$), each of rate λ. N_0 and N are linked through $N_0 = N + \sqrt{c}(1 - N)$, $0 \leq c \leq 1$, thus introducing a correlation measure c. The probability that an event of set $\{A\}$ will be redistributed across k events in set $\{B\}$, follows a binomial distribution

$$\rho_k(N, N_0) = \binom{N}{k} \left(\frac{1}{N_0}\right)^k \left(1 - \frac{1}{N_0}\right)^{N-k}, \quad (1)$$

$k = 0, \ldots, N$. Here, $1/N_0$ emerges as the ratio between the average number of uniform random assignments of events in $\{A\}$ to events in $\{B\}$ (N/N_0, equaling the
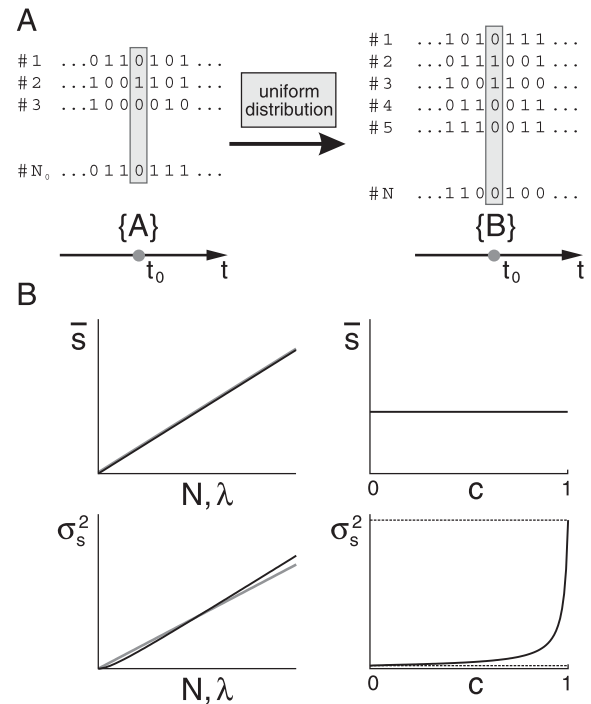
Fig. 2. Temporal correlation in the multiple input channels was introduced using a distributed generator algorithm (A), in which, at each time t_0, the activity pattern $\{A\}$ of N_0 independent channels was redistributed among N input channels (set $\{B\}$). The mean $\overline{s}$ shows a linear dependence on N and λ, and is independent on c. The variance σ_s^2 is linear in λ (B, left, grey) but depends nonlinearly on the number of input channels N (B, left, black) and correlation c (B, right) of the multi-channel inputs. Dashed lines show the asymptotic values of σ_s^2 for $N \to \infty$ in the case of $c = 0$ and $c = 1$.

average number of events in $\{B\}$ assigned to each element of $\{A\}$) and the total number N of events in $\{B\}$. The mean number of random assignments is given by $\overline{k} = \sum_{k=0}^{N} \rho_k(N, N_0)k = N/N_0$, which equals the average number of times each event of set $\{A\}$ is redistributed among elements of $\{B\}$. Equivalently, the variance of random assignments is given by $\sigma_k^2 = N(N_0 - 1)/N_0^2$. Furthermore, it can be shown that this correlated activity has an instantaneous pairwise correlation coefficient of $1/N_0 = 1/(N + \sqrt{c}(1 - N))$ (see also Ref. [20]).

In order to apply Campbell's theorem in the case of multiple correlated input channels as described above, we construct a new shot noise process based on the following two assumptions: first, the time course of k co-releasing identical quantal events $h_k(t)$ equals the sum of k quantal time courses: $h_k(t) = kh_1(t)$, $h_1(t) \equiv h(t)$. Second, the output $s(t)$ due to N correlated Poisson processes equals the sum over the time course of k ($k = 0, \ldots, N$) co-releasing identical quantal events stemming from N_0 independent Poisson trains. For each of the N_0 independent Poisson trains, this sum is weighted according to a binomial distribution (Eq. (1)). Mathematically, this process is equivalent to a shot noise process $s(t) = \sum_j A_j h(t - t_j)$ with amplitude A_j given by an independent random

variable taking values $k = 0, \ldots, N$ with the distribution given in equation (1), and t_j arising from a Poisson process with rate $N_0 \lambda$.

With this, the mean $\overline{s}$ and variance σ_s^2 of multiple correlated shot noise processes are given by

$$\overline{s} = \lambda N_0 \sum_{k=0}^{N} \rho_k(N, N_0) \int_{-\infty}^{\infty} dt\, h_k(t), \qquad (2)$$

$$\sigma_s^2 = \lambda N_0 \sum_{k=0}^{N} \rho_k(N, N_0) \int_{-\infty}^{\infty} dt\, h_k(t)^2. \qquad (3)$$

3 Statistical characterization of multichannel shot noise systems

In order to investigate in detail the impact of correlation in the multi-channel inputs, we considered the example of an exponential quantal response function $h(t) = h_0 e^{-t/\tau}$, $t \geq 0$ ($h(t) \equiv 0$, $t < 0$), where τ denotes the time constant and h_0 the maximal response for each channel. With this, the cumulants C_n, $n \geq 1$, of a multi-channel shot noise process read

$$C_n := \lambda N_0 \sum_{k=0}^{N} \rho_k(N, N_0) \int_{-\infty}^{\infty} h_k^n(t) dt \qquad (4)$$

$$= \frac{\lambda \tau h_0^n}{n} \sum_{k=0}^{N} \binom{N}{k} k^n \frac{((N-1)(1-\sqrt{c}))^{N-k}}{(N + \sqrt{c}(1-N))^{N-1}}.$$

In particular, the mean and variance (C_1 and C_2, respectively) are given by:

$$\overline{s} = \lambda N h_0 \tau, \qquad (5)$$

$$\sigma_s^2 = \frac{1}{2} \lambda N h_0^2 \tau \left(1 + \frac{N-1}{N + \sqrt{c}\,(1-N)} \right). \qquad (6)$$

The method for introducing temporal correlation in the multi-channel input pattern preserves the total release rate λN. This directly translates into the independence of the mean on the correlation measure c, whereas $\overline{s}$ is linearly dependent on λ and N (Fig. 2B). The variance σ_s^2 shows a monotonic but nonlinear dependence on c and N, being proportional to $\lambda N (1 + \frac{N-1}{N + \sqrt{c}\,(1-N)})$. For vanishing correlation ($c = 0$), σ_s^2 approaches a value proportional to $2\lambda N$ for large N. Note that for zero correlation the system is still equivalent to a shot noise process of rate $\lambda N = \lambda N_0$, as can be inferred from the mean $\overline{s}$, but a factor $2\lambda N$ resulting from the used shuffling algorithm enters now the variance σ_s^2. On the other hand, for maximal correlation ($c = 1$), there is only one independent input channel, in which case $\sigma_s^2 \sim \lambda N^2$ (Fig. 2B). The analytic values for $\overline{s}$ and σ_s^2 were compared with corresponding results from numerical simulations, and showed an excellent agreement in the whole investigated parameter range ($100 \leq N \leq 10,000$; $0.1 \leq \lambda \leq 5$ Hz; $0 \leq c \leq 1$; relative error $<1\%$ due to limited numerical statistics).

Although equations (5) and (6) describes the functional dependence of the mean $\overline{s}$ and variance σ_s^2 for a system with exponential response functions triggered by correlated multi-channel shot noise processes, equations (2) and (3) are general expressions which can be applied to other response function and notions of correlation among multiple inputs as well. Indeed, the mean (or variance) of a systems output is calculated as finite weighted sums of integrals over quantal response functions (or their squared) which describe the response triggered by a correlated inputs. Whereas this integral only depends on the kinetics of the response elicited by co-releasing events, the weighting factor only depends on the input statistics, in particular the strength of correlation. For a strictly monotonic dependence between the number of co-releasing events and the resulting response, e.g. an increase in the quantal amplitude with the number of triggering correlated inputs, $\overline{s}$ and σ_s^2 will always show a strictly monotonic dependence on the correlation c. The advantage of the chosen exponential response and notion of correlation is that the integral over the release kinetics, and sum over the input statistics can be performed explicitly. In addition, for many processes in nature, such as for instance synaptic transmission, an exponential response function provides a sufficiently good approximation.

Equations (5) and (6) are sufficient to deduce the rate λ and correlation c from the lowest order statistical analysis of the system's output. However, more information about quantal response function and statistics of the multiple input channels can be obtained from a full statistical characterization, including the correlation functions and amplitude distribution. The explicit expression for the correlation function $C(t_1, t_2)$ and autocorrelation function $C(T) := C(T, 0)$ of a multi-channel shot noise process $s(t)$ is

$$C(t_1, t_2) := \lambda N_0 \sum_{k=0}^{N} \rho_k(N, N_0) \int_{-\infty}^{\infty} h_k(t - t_1) h_k(t - t_2) dt$$

$$= \frac{1}{2} \lambda \tau h_0^2 N \left(1 + \frac{N-1}{N + \sqrt{c}(1-N)} \right) e^{\frac{|t_2 - t_1|}{\tau}}. \quad (7)$$

In a similar fashion, the moments M_n, $n \geq 1$, of the shot noise process $s(t)$, defined by $M_n = \int_{-\infty}^{\infty} s(t)^n dt$, can be deduced, yielding the finite sum

$$M_n = \sum_{k=1}^{n} \sum_{(n_1, \ldots, n_k)} \frac{n!}{k! n_1! \cdots n_k!} C_{n_1} \cdots C_{n_k}, \qquad (8)$$

where the second sum denotes the partition of n into a sum over k integers $n_i \geq 1$, $1 \leq i \leq k$.

From the real part of the Fourier-transform of the moment generating function

$$Q_s(u) := \exp \left[-\lambda N_0 \sum_{k=0}^{N} \rho_k(N, N_0) \int_{-\infty}^{\infty} \left\{ 1 - e^{-u h_k(t)} \right\} dt \right],$$

$$(9)$$

the amplitude probability distribution $\rho_s(h)$ can be calculated. A lengthy but straightforward calculation yields

$$\rho_s(h) = \frac{1}{\sqrt{2\pi C_2}}\, e^{-\frac{(C_1-h)^2}{2C_2}}$$

$$+ \sum_{m=1}^{\infty}\sum_{k=0}^{\infty} \frac{(-2)^{m-k+1}}{\sqrt{2\pi}\,k!}\frac{\Gamma[3/2+m+k]}{\Gamma[1/2+k]}$$

$$\times \frac{(C_1-h)^{2k}}{C_2^{3/2+m+k}}\left(\frac{C_1-h}{1+2k}d_{2m+1}+d_{2m+2}\right). \quad (10)$$

Here, $d_n = \sum_{k=1}^{[\frac{n}{3}]}\sum_{(n_1,\ldots,n_k)}\frac{C_{n_1}\cdots C_{n_k}}{k!n_1!\cdots n_k!}$, where the second sum runs over all partitions of n into a sum of k terms $n_i \geq 3$, $1 \leq i \leq [\frac{n}{3}]$, $n \geq 3$.

The double infinite sum in equation (10) does not allow a closed analytic expression for the amplitude distribution of a correlated multi-channel shot noise process. In lowest order, $\rho_s(h)$ takes a symmetric Gaussian form (Fig. 3A, dashed). At higher orders, a polynomial in h with coefficients given by rational functions of the cumulants is responsible for corrections leading to an asymmetric distribution. Considering corrections up to third order in h, $\rho_s(h)$ is given by

$$\rho_s(h) = \frac{1}{\sqrt{2\pi C_2}}\, e^{-\frac{(C_1-h)^2}{2C_2}}$$

$$\times \left(1 - \frac{C_3(C_1-h)(C_1^2-3C_2-2C_1h+h^2)}{6C_2^3}\right), \quad (11)$$

which fits well the real distribution for corresponding parameter values even for strong asymmetries (Fig. 3A, black solid). The level of asymmetry increases with decreasing ratio $C_1/\sqrt{C_2} \equiv \overline{s}/\sigma_s$, whereas for $\lambda N \to \infty$ and small c the distribution takes a nearly Gaussian shape (Fig. 3B).

Finally, the power spectral density of a multi-channel shot noise process with exponential quantal response function

$$S_s(\nu) = \lambda N_0 \sum_{k=0}^{N}\rho_k(N,N_0)|H_k(\nu)|^2, \quad (12)$$

where $H_k(\nu) = \int_{-\infty}^{\infty}h_k(t)e^{-2\pi i\nu t}dt$, is given by

$$S_s(\nu) = \lambda N\left(1 + \frac{N-1}{N+\sqrt{c}(1-N)}\right)\frac{h_0^2\tau^2}{1+(2\pi\nu\tau)^2}, \quad (13)$$
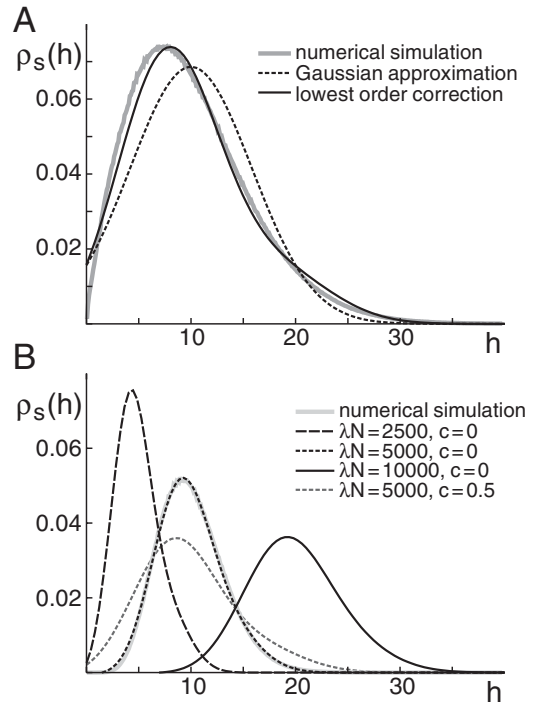
and shows a Lorentzian behavior

$$S(\nu) = \frac{2D\tau^2}{1+(2\pi\tau\nu)^2}$$

(Fig. 4A). Whereas the frequency dependence remains unaltered by the correlation c, the total rate λ or number of input channels N, the maximal power is proportional to

$$D = \frac{1}{2}\lambda N h_0^2\left(1 + \frac{N-1}{N+\sqrt{c}(1-N)}\right)$$

and a nonlinear monotonic function of c and N (Fig. 4B).

Fig. 3. Amplitude probability distribution for multiple correlated input channels. $\rho_s(h)$, equation (10), shows a generally asymmetric behavior (A, grey), which can be approximated by the lowest order correction (A, black solid) to the corresponding Gaussian distribution (A, black dashed). The amplitude distribution depends on c and the total rate, and approaches a Gaussian for high total input rates or small correlations (B). Parameters: $N = 100$, $\lambda = 50$ Hz, $c = 0.7$ (A); $h_0 = 1$, $\tau = 2$ ms in all cases.
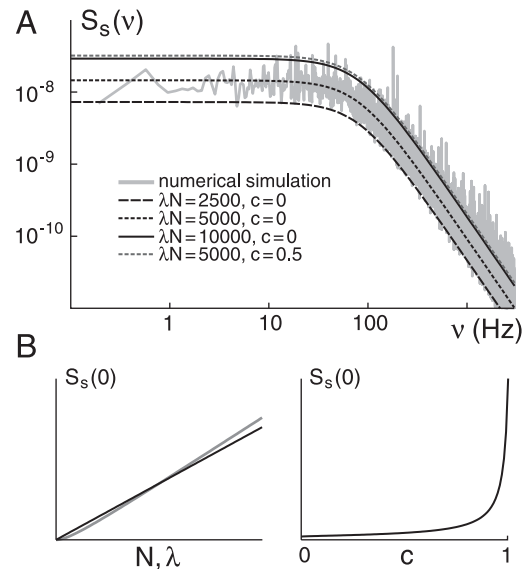

Fig. 4. The power spectral density of a shot noise process with multiple correlated input channels and exponential quantal response function shows a Lorentzian behavior (A). The total power depends on both, the number of input channels N (B, left, black), rate λ (B, left, grey) and the level of correlation c (B, right) of the multi-channel inputs. Parameters: $h_0 = 1$, $\tau = 2$ ms.

4 Parameter estimation

The relations given in the previous section allow to characterize multi-channel shot noise processes from experimental recordings. The mean $\overline{s} \equiv C_1$ and variance $\sigma_s^2 \equiv C_2$ of the amplitude distribution (Eqs. (5) and (6), respectively) are monotonic functions of c and λ (see Fig. 2B), thus allowing to estimate those parameters from experimentally-obtained distributions for which $\overline{s}$ and σ_s^2 are known. Here, in order to obtain faithful estimates, the total number of input channels N as well as the quantal decay time constant and amplitude, τ and h_0, respectively, need to be known. Average values for N can be obtained from detailed morphological studies (see e.g. [24]). Estimates for the quantal conductance h_0 and synaptic time constant τ can be obtained using whole cell recordings of miniature synaptic events (see e.g. [22]). Average values for the synaptic time constants are also accessible through fits of the power spectral density obtained from current-clamp recordings, as shown in [23,27]. Finally, the explicit expression for $S_s(\nu)$ (Eq. (13)), can be used to fit experimental power spectral densities obtained from voltage-clamp recordings, yielding values for the time constant τ and the power coefficient D.

We tested this paradigm in numerical simulations of various models of cortical neurons with multiple synaptic inputs, in which the temporal correlation c and average release rate at single synaptic terminals λ were changed in a broad parameter regime. Values for the mean $\overline{s}$ and variance σ_s^2 of excitatory and inhibitory synaptic conductances can independently be obtained either by using a voltage-clamp protocol [25], or a protocol which makes use of current-clamp recordings [26]. Both approaches yield the same estimates for the mean and variance of excitatory and inhibitory conductances. In what follows we, therefore, restrict to conductance estimates obtained with the voltage-clamp protocol. With values available for the mean and variance for both excitatory and inhibitory synaptic conductances, equations (5) and (6) will be utilized to characterize statistical properties, in particular c and λ, independently for excitatory and inhibitory synaptic terminals.

First, we investigated a single-compartment neuronal models with multiple excitatory and inhibitory synaptic terminals (Fig. 5). Here, the synaptic conductances from individual terminals are lumped together and determine the output of the system. The estimated values for the average release rate λ matched nearly exact the known input values for both excitatory and inhibitory synapses (Fig. 5, top). A good agreement was also obtained for estimates of the correlation c (Fig. 5, bottom), although a small systematic underestimation was observed. The latter can be attributed to statistical limitations of the available conductance estimates (recordings were performed over finite time with limited temporal resolution) as well as deviations of the conductance distributions from the Gaussian shape (only in the limit case of infinite input rate the distributions are expected to be Gaussian; see Eqs. (10) and (11)).
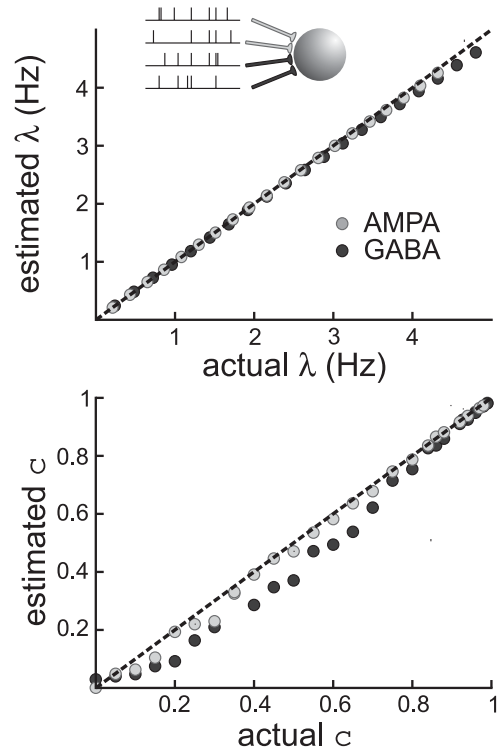
Fig. 5. Estimation of λ (top) and c (bottom) from the characterization of the total conductance distribution for different levels of network activity in a single-compartment neuronal model with multiple excitatory (*AMPA*, $N = 4472$, quantal conductance 1.2 nS) and inhibitory (*GABA*, $N = 3801$, quantal conductance 0.6 nS) synaptic inputs (inset). Estimated values are shown as functions of the actual values used for the numerical simulations. Excellent estimates were obtained for λ, whereas estimates for c slightly underestimated the actual value. Neuronal simulations of 100 s duration with time resolution of 0.1 ms were performed.

A qualitatively different result was obtained when synaptic terminals were distributed over a spatially extended dendritic tree. In such a biophysical model of a morphologically reconstructed neuron (Fig. 6, inset), a marked but systematic underestimation of both the average release rate (Fig. 6, top) as well as the correlation between multiple synaptic terminals (Fig. 6, bottom) was obtained. Further investigation revealed that this underestimation of λ and c can be attributed to the attenuation of synaptic inputs along the spatially extended dendritic structure. Here, distal synaptic input will have markedly lower impact on the somatic recording site than more proximal inputs (Fig. 7A, left), despite the fact that all synapses had the same quantal conductance and kinetics.

To estimate and characterize this attenuation, "ideal" voltage-clamp simulations were performed to estimate the conductance "seen" at the soma for individual excitatory synaptic events (Fig. 7A, right). The amplitude and integral of the obtained somatic conductance transients decreased with path distance of the synaptic stimulus. As
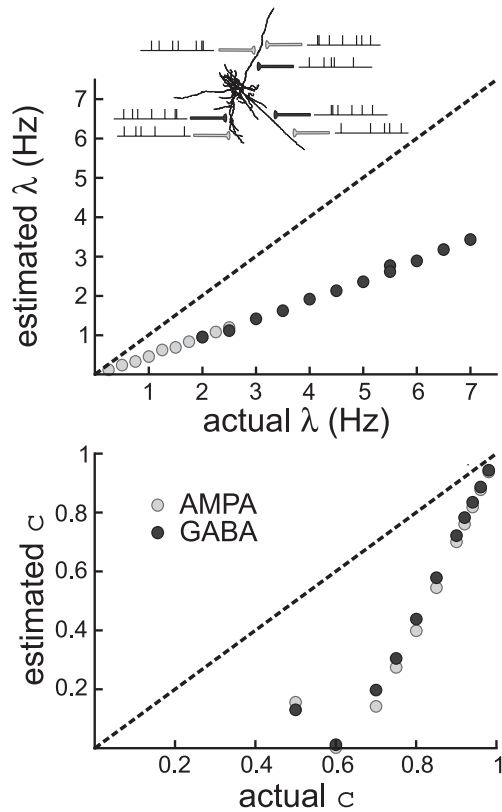
Fig. 6. Estimation of the average channel rate λ (top) and correlation c (bottom) from recorded conductance distribution for different levels of activity at multiple spatially distributed excitatory ($AMPA$, $N = 16563$, quantal conductance 1.2 nS) and inhibitory ($GABA$, $N = 3376$, quantal conductance 0.6 nS) synaptic terminals in a detailed biophysical neuronal model of a morphologically reconstructed cortical neuron (inset). Estimated values are shown as functions of the actual values used for the numerical simulations. In contrast to the single-compartment model (Fig. 5), dendritic filtering in this multi-compartment model caused a severe underestimation of λ and c. Neuronal simulations of 100 s duration with time resolution of 0.1 ms were performed.

a first approximation incorporating this dendritic filtering effect, we averaged the conductance contribution from individual synaptic inputs over the path distance (Fig. 7A, right bottom, dashed line). This leads to a correction in the estimation of the rate and correlation (Fig. 7B) so that estimated values for different levels of network activity, in particular λ, match now much better with the actual values used for the numerical simulations. More sophisticated models incorporating dendritic filtering include the distribution of synapses across the dendritic tree, and are currently under investigation, also with respect to their applicability in experiments [27].

The obtained results suggest that, due to the dependencies of the mean and variance of synaptic conductances, multi-channel shot noise processes open a potential way to quantitatively assess the frequency (and number; not shown) of synaptic input channels as well as their temporal correlation. This would not just allow to charac-
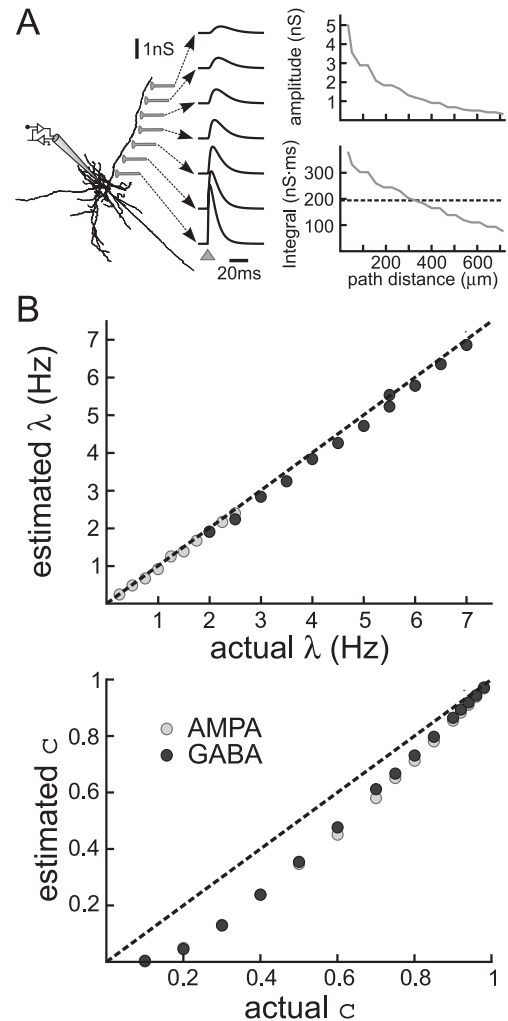
Fig. 7. Estimation of λ (B, top) and c (B, bottom) from recorded excitatory ($AMPA$) and inhibitory ($GABA$) conductance distribution for different levels of network activity in a detailed biophysical model of a morphologically reconstructed cortical neuron (same model as in Fig. 6) under incorporation of a simple model of dendritic filtering (A; quantal conductance 12 nS; see text for explanation). This yields an excellent estimation for the average rate at synaptic terminals, whereas estimations for c show still a systematic lower value which, however, is markedly reduced compared to the case without incorporating the effect of dendritic filtering. For the estimates, the same dataset as in Figure 6 was used.

terize the statistical properties of the multisynaptic inputs to single cells, but also to infer properties of the activity in the embedding network from recordings of single-cell activity.

5 Limits of the method and future directions

The method outlined here proposes a characterization of the statistics of synaptic inputs distributed across a spatially extended dendritic structure. This method should be viewed as a first step to assess the statistical properties of

network activity based on the sole knowledge of single-cell activity. To date, only technically sophisticated multisite extracellular recordings or imaging allow to quantify network dynamics on a larger scale. The approach presented here applies to intracellular recordings of single neurons and could complement such multisite recordings.

However, in order to obtain reliable estimates of network correlation or average rates from intracellular data, some details need to be resolved which still limit the applicability of the proposed method. The main limitations arise from the fact that synaptic inputs are spatially distributed across an extended dendritic structure. Dendritic filtering affecting the transmission of signals to the somatic recording site, which in general will be spatially separated from the site of the synaptic inputs, modifies the signal and, thus, the obtained estimates. This modification depends not only on the exact morphology of the dendritic structure, but also on the distribution of synaptic terminals. In the simplest case of a uniform density and known cellular morphology, good estimates can be obtained along the lines described in the previous section (see Fig. 7). However, in most cases the morphology of the dendritic tree is not known, as is the number of synaptic terminals and their distribution. Available detailed morphological studies and 3-dimensional cellular reconstructions can, at least to some extent, reduce those uncertainties.

The value of conductance per synaptic terminal may vary across the dendritic structure, as found for example in hippocampal pyramidal neurons whose conductances are scaled according to their distance to soma to compensate for dendritic filtering [28] (but see [29]; a similar conductance scaling does not seem to apply to neocortical neurons [30]). In the case of a functionally known conductance scaling, e.g. a known quantal synaptic conductances as function of the distance from the soma obtained by fitting experimental data, both the quantal time course $h_k(t)$ as well as the probability of its occurrence $\rho_k(N, N_0)$ will not only be a function of the number of co-releasing terminals k (as well as N and N_0), but also the distance from the somatic recording site. Equations (2)–(4), (7), (9) and (12) will then contain additional sums (or integrals in the large N limit) over the location of synaptic terminals. This approach was used in the previous section to average over the contribution of synaptic conductances, spatially distributed with uniform density and of equal quantal amplitude, to the activity at the somatic recording site.

Another main limitation concerns the exact nature of the correlations that are extracted by the present method. We assumed that correlations are constant in time, that they are instantaneous (i.e., peaked at time zero), and we neglected correlations between excitatory and inhibitory inputs. In reality, temporal correlations are dynamic, they may occur over finite times, and there may be correlations between excitatory and inhibitory inputs. The present method characterizes the "average" correlation and cannot resolve temporal variations. However, the latter can be obtained by averaging over successive trials, or by applying the method within successive time windows. The number of trials and the temporal signature of the involved biophysical processes, as well as the mathematical tools utilized for the statistical description of the single cell activity, will set an upper limit for the temporal resolution with which correlations can be extracted. Reliable estimates of the mean and variance of synaptic conductances can be obtained from several thousand recorded data points, which will yield an upper limit for the temporal resolutions of a few hundred millisecond for single trials, and tens of milliseconds for multiple trials if standard electrophysiological recording protocols are used.

Concerning finite-time correlation and excitatory-inhibitory correlations, including such effects will necessarily change the functional form of the quantal time course $h_k(t)$ as well as the probability of its occurrence $\rho_k(N, N_0)$. This type of extension will be the subject of future work. However, despite those limitations, the approach described here is a simple and extendable approach, which highlights the potential usefulness of a natural extension of the original shot noise formalism.

6 Discussion

We have shown that systems with multiple correlated input channels can be treated within the context of shot noise stochastic processes, leading to analytic expressions for the mean and standard deviation of the system's stochastic output. In cerebral cortex, every neuron receives thousands of synaptic inputs from other neurons, and the seemingly random activity of these inputs causes large fluctuations of the total membrane conductance [21]. By describing this system as a multi-channel shot noise process, it should be possible to relate the statistics of conductance fluctuations with the kinetics and the correlation of synaptic inputs. This procedure could yield methods to estimate, from single-neuron activity, temporal modulations of correlations among the discharge of a large number of neurons, which, although of prime physiological importance, still remains an uncharacterized parameter.

References

1. N. Campbell, Proc. Cambr. Phil. Soc. **15**, 117 (1909); 310 (1909)
2. W. Schottky, Ann. Phys. (Leipzig) **57**, 541 (1918)
3. S.O. Rice, Bell Syst. Tech. J. **23**, 282 (1944); S.O. Rice, Bell Syst. Tech. J. **24**, 46 (1945)
4. M.B. Johnson, Phys. Rev. **29**, 367 (1927); H. Nyquist, Phys. Rev. **32**, 110 (1928)
5. A. Papoulis, *Probability, random variables, and stochastic processes* (McGraw-Hill, Boston, USA, 1991)
6. E.N. Gilbert, H.O. Pollak, Bell Syst. Tech. J. **39**, 333 (1960)
7. A. Papoulis, J. Appl. Prob. **8**, 118 (1971)

8. G.M. Morris, J. Opt. Soc. Amer. A **1**, 482 (1984); A.O. Hero, IEEE Trans. Inform. Theory **37**, 92 (1991)

9. T.T. Kadota, IEEE Trans. Inform. Theory **34**, 1517 (1988); C.W. Helstrom, C.-L. Ho, IEEE Trans. Commun. **40**, 1327 (1992)

10. L. Saminadayar et al., Phys. Rev. Lett. **79**, 2526 (1997); R. de-Picciotto et al., Nature **389**, 162 (1997)

11. M.J.M. de Jong, C.W.J. Beenakker, in *Mesoscopic Electron Transport*, edited by L.L. Sohn et al., 225 (Kluwer Academic Publishers, Dordrecht, 1997); Ya.M. Blanter, M. Büttiker, Phys. Rep. **336**, 2 (2000)

12. J.C. Cuevas et al., Phys. Rev. Lett. **82**, 4086 (1999); R. Cron et al., Phys. Rev. Lett. **86**, 4104 (2001); J.C. Cuevas, M. Fogelström, Phys. Rev. Lett. **89**, 227003 (2002)

13. J.C. Egues et al., in *Quantum Noise in Mesoscopic Physics*, NATO ASI Series II, Vol. 97 (Kluwer Academic Publishers, Dordrecht, 2003)

14. S.B. Lowen, M.C. Teich, IEEE Trans. Inform. Theory **36**, 1302 (1990)

15. C.W.J. Beenakker, M. Patra, Mod. Phys. Lett. B **13**, 337 (1999)

16. C. Klüppelberg, T. Mikosch, Bernoulli **1**, 125 (1995); G. Samorodnitsky, in *Proc. Intern. Conf. on App. Prob. and Time Series*, edited by R.P. Heyde et al., p. 322 (Springer Verlag, 1995)

17. F. Baccelli, B. Blaszczyszyn, Adv. Appl. Probab. **33**, 293 (2001)

18. M.C. Teich, B.E.A. Saleh, J. Opt. Soc. Am. **71**, 771 (1981); B.E.A. Saleh, M.C. Teich, Biol. Cybern. **52**, 101 (1985); M.C. Teich et al., J. Opt. Soc. Am. A **14**, 529 (1997); M.A. Freed, J. Neurosci. **20**, 3956 (2000); N. Hohn, A.N. Burkitt, Phys. Rev. E **63**, 031902 (2001)

19. A. Destexhe, D. Paré, J. Neurophysiol. **81**, 1531 (1999); M. Rudolph, A. Destexhe, Phys. Rev. Lett. **86**, 3662 (2001)

20. R. Gütig et al., J. Neurosci. **23**, 3697 (2003)

21. A. Destexhe, M. Rudolph, D. Paré, Nature, Rev. Neurosci. **4**, 739 (2003)

22. H. Markram et al., J. Physiol. **500**, 409 (1997); P. Salin, D.A. Prince, J. Neurophysiol. **75**, 1573 (1996); P. Stern et al., J. Physiol. **449**, 247 (1992)

23. A. Destexhe, M. Rudolph, J. Comput. Neurosci. **17**, 327 (2004)

24. J. DeFelipe et al., Neurocytology **31**, 299 (2003)

25. A. Destexhe et al., Neurosci. **107**, 13 (2001)

26. M. Rudolph, A. Destexhe, Neural Comput. **17**, 2301 (2005)

27. M. Rudolph et al., J. Neurophysiol. **94**, 2805 (2005)

28. J.C. Magee, E.P. Cook, Nature Neurosci. **3**, 895 (2000); B.K. Andrásfalvy, J.C. Magee, J. Neurosci. **21**, 9151 (2001)

29. M. London, I. Segev, Nature Neurosci. **4**, 853 (2001)

30. S.R. Williams, G.J. Stuart, Science **295**, 1907 (2002)